

Supplementary material

# Geomorphology, Mineralogy, and Geochronology of Mare Basalts and Non-Mare Materials Around the Lunar Crisium Basin

Xuejin Lu<sup>1</sup>, Haijun Cao<sup>1</sup>, Zongcheng Ling<sup>1,2\*</sup>, Xiaohui Fu<sup>1</sup>, Le Qiao<sup>1</sup> and Jian Chen<sup>1</sup>

<sup>1</sup> Shandong Key Laboratory of Optical Astronomy and Solar-Terrestrial Environment, School of Space Science and Physics, Institute of Space Sciences, Shandong University, Weihai 264209, China.

<sup>2</sup> CAS Center for Excellence in Comparative Planetology, Chinese Academy of Sciences, Hefei 230026, China.

\* Correspondence: zcling@sdu.edu.cn (Zongcheng Ling)

## Figure and Table Captions

**Figure S1** (a) Four spectra from high-Ti region are smoothed and continuum-removed. Three dashed lines are the absorption centers of olivine near 900 nm, 1050 nm, and 1200 nm respectively. (b) The positions of spectrum A. (c) The positions of spectrum B, C, and D. Red pixels contain >9 wt.% TiO<sub>2</sub> content.

**Figure S2** The chronology of Mare Crisium from (a) Boyce et al. (1978) [9] and (b) Hiesinger et al. (2011) [10]. Different colors represent specific ages. Colder colors are younger and warmer are older. The green star denotes Luna 24 landing site at the southern Crisium basin.

**Figure S3** The highland units are sketched in this study. (a) There are two group units: Imbrium Group (in green) and Crisium Group (in blue). Two magnified view of northwestern portion (b) and southwestern portion (c) are shown to illustrate features of these highland units.

**Table S1** Information of Moon Mineralogy Mapper(M<sup>3</sup>) datasets used in this study.

**Table S2** The calculation formula and definition of spectra parameters used in this study.

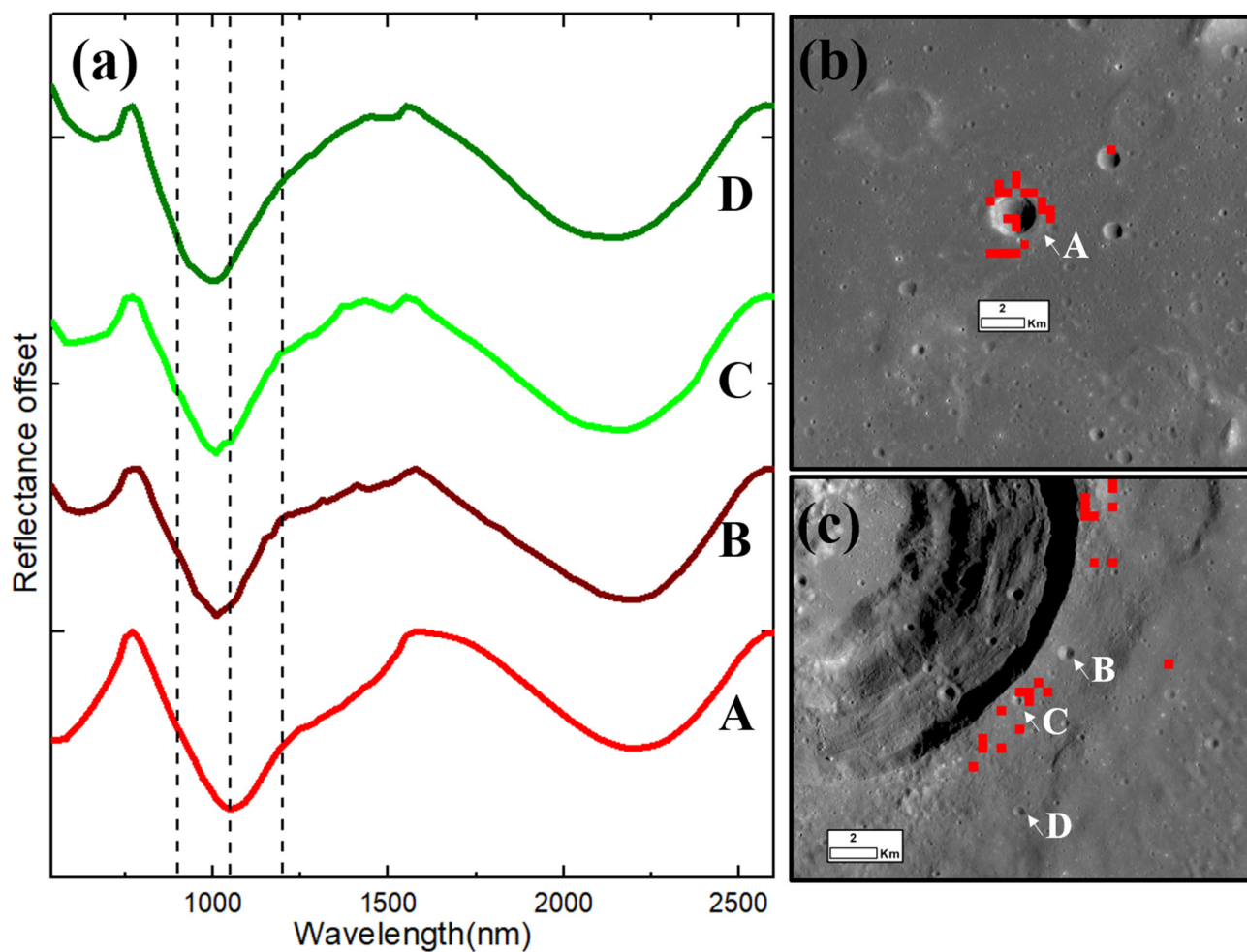


**Figure S1.** (a) Four spectra from high-Ti region are smoothed and continuum-removed. Three dashed lines are the absorption centers of olivine near 900 nm, 1050 nm, and 1200 nm respectively. (b) The positions of spectrum A. (c) The positions of spectrum B, C, and D. Red pixels contain >9 wt.% TiO<sub>2</sub> content.

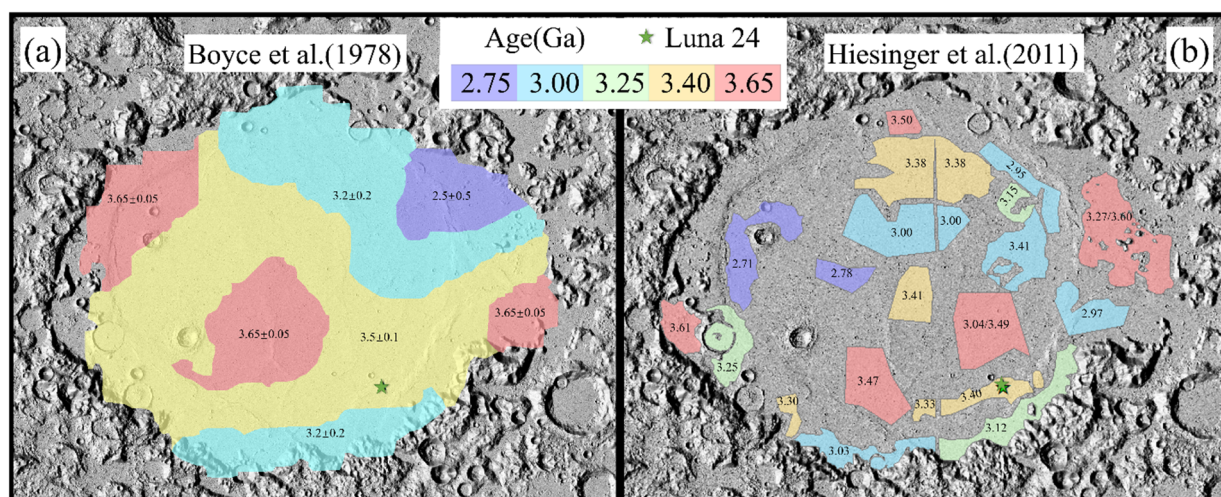


**Figure S2.** The chronology of Mare Crisium from (a) Boyce et al. (1978) [9] and (b) Hiesinger et al. (2011) [10]. Different colors represent specific ages. Colder colors are younger and warmer are older. The green star denotes Luna 24 landing site at the southern Crisium basin.

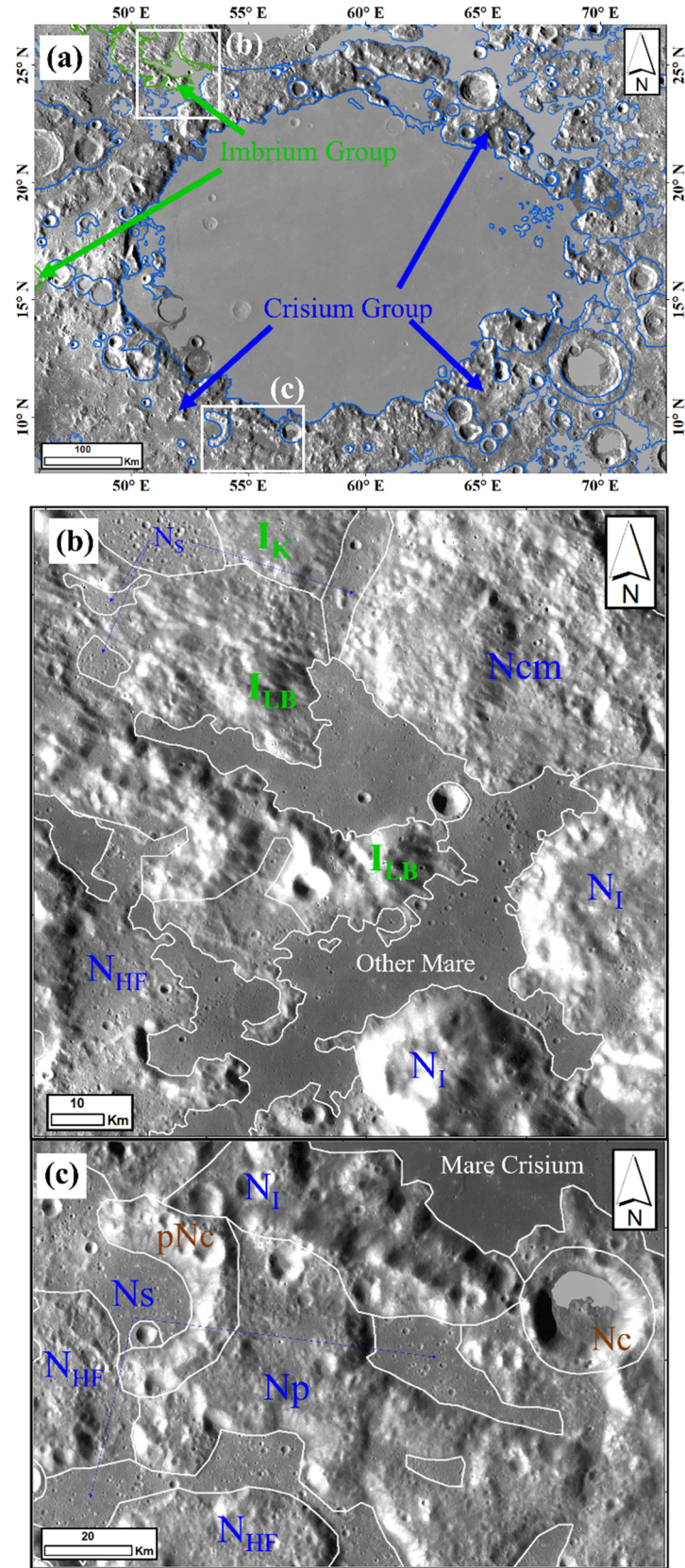


**Figure S3.** The highland units are sketched in this study. (a) There are two group units: *Imbrium Group* (in green) and *Crisium Group* (in blue). Two magnified view of northwestern portion (b) and southwestern portion (c) are shown to illustrate features of these highland units.

**Table S1.** Information of Moon Mineralogy Mapper(M<sup>3</sup>) datasets used in this study.

No.	Data File Name	Date	Optical Period	Orbit Altitude (km)	Resolution (m/pixel)
1	M3G20090131T091031_V01_RFL	31-January-2009	OP1B	100	140
2	M3G20090602T203342_V01_RFL	2-June-2009	OP2C	200	280
3	M3G20090603T010112_V01_RFL	3-June-2009	OP2C	200	280
4	M3G20090603T050442_V01_RFL	3-June-2009	OP2C	200	280
5	M3G20090603T134223_V01_RFL	3-June-2009	OP2C	200	280
6	M3G20090603T174502_V01_RFL	3-June-2009	OP2C	200	280
7	M3G20090603T221232_V01_RFL	3June-2009	OP2C	200	280
8	M3G20090604T023806_V01_RFL	4-June-2009	OP2C	200	280
9	M3G20090604T064302_V01_RFL	4-June-2009	OP2C	200	280
10	M3G20090604T104552_V01_RFL	4-June-2009	OP2C	200	280
11	M3G20090604T151322_V01_RFL	4-June-2009	OP2C	200	280
12	M3G20090604T191631_V01_RFL	4-June-2009	OP2C	200	280
13	M3G20090604T195758_V01_RFL	4-June-2009	OP2C	200	280
14	M3G20090604T234352_V01_RFL	4-June-2009	OP2C	200	280
15	M3G20090605T040250_V01_RFL	5-June-2009	OP2C	200	280
16	M3G20090605T081431_V01_RFL	5-June-2009	OP2C	200	280



**Table S2.** The calculation formula and definition of spectral parameters used in this study.

Spectral parameter	Formula	Definition	Reference
Band center I	$\begin{aligned} & x_{1000} \\ & = [Bn1000_{min} \\ & \quad - 5: Bn1000_{min} + 5] \\ & \text{BC I} \\ & = \text{wavelength}\{\min[\text{polyfit}(x_1) \end{aligned}$	<p>The wavelength corresponding the minimum value of the second-order polynomial fit at 1,000 nm</p>	[1] [2]
Band center II	$\begin{aligned} & x_{2000} \\ & = [Bn2000_{min} \\ & \quad - 8: Bn2000_{min} + 8] \\ & \text{BC I} \\ & = \text{wavelength}\{\min[\text{polyfit}(x_2) \end{aligned}$	<p>The wavelength corresponding the minimum value of the second-order polynomial fit at 2,000 nm</p>	
IBD 1000	$\text{IBD 1000} = \sum_{n=\text{first shoulder}}^{\text{middle shoulder}} 1 - R_c(n)$	<p>The first shoulder at 660~930 nm The middle shoulder at 1,109~2,018 nm (<math>R_c = \text{continuum removed reflectance}</math>)</p>	[3] [4]
IBD 2000	$\text{IBD 2000} = \sum_{n=\text{middle shoulder}}^{\text{last shoulder}} 1 - R_c(n)$	<p>The middle shoulder at 1,109~2,018 nm The last shoulder at 2600 nm (<math>R_c = \text{continuum removed reflectance}</math>)</p>	
IBDR	$\text{IBDR} = \frac{\text{IBD 2000}}{\text{IBD 1000}}$	The ratio of IBD 2000 and IBD 1000	[5] [6]
HCP/LCP	$\begin{aligned} & \frac{\text{HCP}}{\text{LCP}} \\ & = \frac{1}{2} \\ & \times \left( \frac{\text{HCP1000nm}}{\text{LCP1000nm}} \right. \\ & \quad \left. + \frac{\text{HCP2000nm}}{\text{LCP2000nm}} \right) \end{aligned}$	<p>The ratios of high-Ca pyroxene and low-Ca pyroxene bands strengths at 1,000nm and 2,000nm, and then take the average of two ratios.</p>	[7] [8]

---

## References

1. Adams, J. B. "Visible and near-infrared diffuse reflectance spectra of pyroxenes as applied to remote sensing of solid objects in the solar system." *Journal of Geophysical Research* 79 (1974): 4829-36. 10.1029/JB079i032p04829.
2. Gaffey, M. J. "Mineralogy of asteroids." Presented at AIP Conference Proceedings, 2011. American Institute of Physics, 1386, 129-69.
3. Clark, R. N. and T. L. J. J. o. G. R. S. E. Roush. "Reflectance spectroscopy: Quantitative analysis techniques for remote sensing applications." 89 (1984): 6329-40.
4. Cheek, L., C. Pieters, J. Boardman, R. Clark, J. Combe, J. Head, P. Isaacson, T. McCord, D. Moriarty and J. J. J. o. G. R. P. Nettles. "Goldschmidt crater and the moon's north polar region: Results from the moon mineralogy mapper (m3)." 116 (2011):
5. Mustard, J. F., C. M. Pieters, P. J. Isaacson, J. W. Head, S. Besse, R. N. Clark, R. L. Klima, N. E. Petro, M. I. Staid and J. M. J. J. o. G. R. P. Sunshine. "Compositional diversity and geologic insights of the aristarchus crater from moon mineralogy mapper data." 116 (2011):
6. Varatharajan, I., N. Srivastava and S. V. J. I. Murty. "Mineralogy of young lunar mare basalts: Assessment of temporal and spatial heterogeneity using m3 data from chandrayaan-1." 236 (2014): 56-71.
7. Sunshine, J. M. and C. M. J. J. o. G. R. P. Pieters. "Estimating modal abundances from the spectra of natural and laboratory pyroxene mixtures using the modified gaussian model." 98 (1993): 9075-87.
8. Ling, Z., L. Qiao, C. Liu, H. Cao, X. Bi, X. Lu, J. Zhang, X. Fu, B. Li, J. J. P. Liu, et al. "Composition, mineralogy and chronology of mare basalts and non-mare materials in von kármán crater: Landing site of the chang'e- 4 mission." 179 (2019): 104741.
9. Boyce, J. and D. Johnson. "Ages of flow units in mare crismum based on crater density." Presented at Lunar and Planetary Science Conference Proceedings, 1977. 8, 3495-502.
10. Hiesinger, H., C. van der Bogert, D. Reiss and M. Robinson. "Crater size-frequency distribution measurements of mare crismum." Presented at Lunar and Planetary Science Conference, 2011. 2179.